Supporting Information

Datta et al. 10.1073/pnas.1424563112

SI Materials and Methods

Animal and Human Subjects. Female New Zealand White rabbits were used for experiments at a weight of 3–3.4 kg, and all procedures were conducted in accordance with the recommendations of the *Guide for the Care and Use of Laboratory Animals* of the NIH (1). The Committee on the Ethics of Animal Experiments of the National Institute of Allergy and Infectious Diseases approved the experiments described herein under protocol LCID-3 (permit issued to NIH Intramural Research Program as A-4149-01), and all efforts were made to provide intellectual and physical enrichment and to minimize suffering. Lung tissue samples from subjects undergoing lung resection surgery for recalcitrant multidrug-resistant TB were collected under protocol (clinicaltrials.gov, protocol NCT00816426) approved by the Institutional Review Board of the National Institute of Allergy and Infectious Diseases and by the institutional review boards of the local hospitals conducting the study in the Republic of Korea. The subjects gave written informed consent to participate in the study and to have their resected tissue used for research.

TB Infection of Animals and Drug Treatment. MTB strain HN878 was grown in M7H9 medium and used to infect rabbits by aerosol as previously described (2). The animals were individually housed in open cages in a biological safety level 3 facility for 10–11 wk to allow pathological symptoms to develop. The animals were randomly assigned to one of three groups destined to be administered 5 mg/kg of bevacizumab (Avastin; Genentech, Inc.) by slow intravascular infusion (3) over 20 min (six animals) or given a sham infusion of saline (four animals). Upon treatment start, the animals were monitored for signs of progressive disease. Animals were imaged before infusion and on day 2 or 7, and they were euthanized the following day. A second experiment was conducted with similar numbers of animals for the analysis of bacterial load and contributed tissue to the histology analysis.

FDG-PET/CT Scanning. [^{18}F]FDG doses (1 mCi/kg) were administered, and scanning was initiated at 80 min postdose, matched within 5 min and 10% activity per animal, respectively, to facilitate quantitative assessment of [^{18}F]FDG-PET uptake parameters. CT scans were exported from the Ceretom workstation (NeuroLogica Corporation) into the Inveon Research Workstation software (IRW; Siemens Preclinical Solutions) provided with the Focus 220 PET scanner and coregistered as described previously (2). Further analysis used both IRW software and Osirix 3.8 64-bit (Pixmeo SARL) and MIM Maestro, version 6.2.7 (MIM Software), for individual lesion analysis of volume, density, and FDG uptake as previously described (2, 4).

Injection with Pimonidazole and Hoechst, and Animal Necropsy. Rabbits were killed at described time points after administration of bevacizumab or a sham dose. Sixteen hours before euthanasia, rabbits were given 30 mg/kg of pimonidazole HCl as described previously (2). Using a venous catheter in the ear, the animals were infused with 2.5 mg/kg of Hoechst (Hoechst33342; Sigma–Aldrich) in saline, sedated 4 min later with a mixture of ketamine/xylazine, and humanely euthanized with pentobarbital sodium for a consistent Hoechst exposure time of 7 min. The lung was perfused in situ with 4% (wt/vol) paraformaldehyde through the left ventricle of the heart to preserve the vasculature. Afterward, the lung, spleen, and any observed lymph nodes were removed aseptically and divided into portions for cryopreservation or paraffin-embedded histology. A second experiment with bevacizumab-treated groups and control groups was conducted for bacterial load determination using standard methods (4). These animals were euthanized 8 d postinfusion.

Immunohistochemistry and Immunofluorescence. Tissues sections were fixed in 4% (wt/vol) neutral buffered paraformaldehyde overnight and then either frozen in vapor phase liquid nitrogen or embedded in paraffin, and 5- to 20-μm sections were cut. The endogenous peroxidase was blocked with the addition of 3% (vol/vol) hydrogen peroxide in protein-blocking solution (PBS) for 12 min. The samples were incubated for 20 min at room temperature with PBS (pH 7.5) containing 5% (vol/vol) normal horse serum and 1% normal goat serum, followed by incubation at 4 °C with primary antibodies [CD31 (1:250; BD Bioscience), αSMA (1:200; Sigma), VEGF (1:1,000; Abcam)] (5). The samples were then rinsed and incubated for 1 h at room temperature with a peroxidase-conjugated secondary antibody. The slides were rinsed with PBS and incubated for 5 min with diaminobenzidine. The sections were then washed three times with distilled water, counterstained with Mayer's hematoxylin, washed once with distilled water, and washed once more with PBS. The slides were mounted with a universal mount and examined with a bright-field microscope.

Image Analysis. Granuloma hypoxia and necrosis were quantified using custom in-house semiautomatic MATLAB (MathWorks) image analysis codes for immunohistochemical (IHC) images; all IHC images were scanned using a Nanozoomer 2.0 HT C9600 Series (Hamamatsu) at 20× (0.456 μm per pixel). The granulomas and any necrotic areas were outlined manually from images of lung sections, and void areas (i.e., alveolar spaces, tissue processing artifacts) were eliminated before quantification of tissue area. Positive pimonidazole staining was automatically quantified as an area fraction after establishing a threshold to exclude background staining. The Hoechst area, intensity, and distribution within granulomas were assessed similarly using immunofluorescent images from an Olympus FV1000 confocal laser scanning microscope, with a nonspecific nuclear stain (Sytox green). Granuloma vessel analysis was performed via custom-built semiautomatic software applications designed specifically for the rabbit and human tissues (Visiopharm). Using IHC stains for CD31 and αSMA, the vessel metrics were quantified via initial automatic selection, with subsequent manual verification/modification. Structures were identified as vessels if they included at least two of the following morphological characteristics: (*i*) elongated endothelial cell nuclei, (*ii*) positive brown staining for CD31, and (*iii*) a visible lumen. Microvessel number, density, fraction, and area were assessed via selection of positive CD31 staining, pericyte area was assessed via selection of positive αSMA staining, and lumen area was quantified if surrounded by CD31 staining and/or elongated nuclei.

Statistical Analysis. The statistical analyses were performed using nonparametric or parametric one-way ANOVA tests as appropriate, with Dunn's or Tukey's post-hoc multiple comparison tests, respectively, for the three experimental groups in Prism 5.0 (GraphPad), and P values were calculated, unless otherwise stated. Values are expressed as means ± SD for PET/CT imaging and bacterial load measures (Fig. S3), and as the SEM for histological analysis (all other figures).

1. Committee on Care and Use of Laboratory Animals (1996) *Guide for the Care and Use of Laboratory Animals* (Natl Inst Health, Bethesda), DHHS Publ No (NIH) 85-23.
2. Via LE, et al. (2008) Tuberculous granulomas are hypoxic in guinea pigs, rabbits, and nonhuman primates. *Infect Immun* 76(6):2333–2340.
3. Lopez ES, Rizzo MM, Croxatto JO, Mazzolini G, Gallo JE (2011) Suramab, a novel antiangiogenic agent, reduces tumor growth and corneal neovascularization. *Cancer Chemother Pharmacol* 67(3):723–728.
4. Via LE, et al. (2012) Infection dynamics and response to chemotherapy in a rabbit model of tuberculosis using [^{18}F]2-fluoro-deoxy-D-glucose positron emission tomography and computed tomography. *Antimicrob Agents Chemother* 56(8):4391–4402.
5. Xu L, Tong R, Cochran DM, Jain RK (2005) Blocking platelet-derived growth factor-D/platelet-derived growth factor receptor beta signaling inhibits human renal cell carcinoma progression in an orthotopic mouse model. *Cancer Res* 65(13):5711–5719.

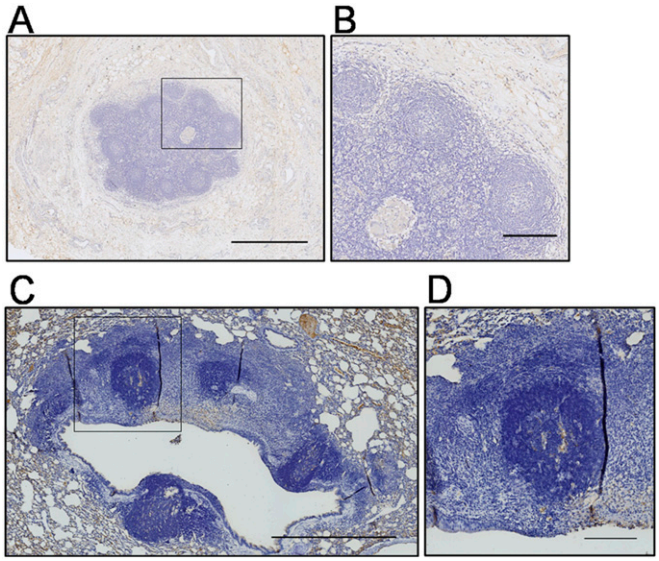

Fig. S1. VEGF is not highly expressed in lymphoid aggregates. VEGF expression (brown) is considerably lower in naturally occurring lymphoid aggregates in apparently unaffected regions of lung tissues from human (*A* and *B*) and rabbit (*C* and *D*) lungs than in similarly sized granulomas in Fig. 1. (Scale bars: *A* and *C*, 1 mm; *B*, 500 μm; *D*, 200 μm.)

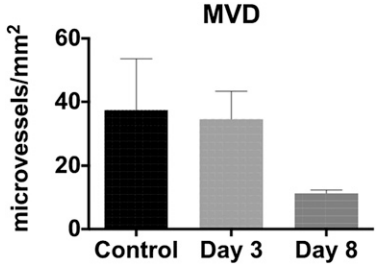

Fig. S2. Bevacizumab treatment does not affect MVD. As described in Fig. 4, vessels were quantified in granulomas in tissue sections from rabbits treated with bevacizumab using semiautomatic Visiopharm software. There is a reduction of MVD (i.e., number of vessels per viable granuloma area, measured in square millimeters) at 3 d and especially 8 d posttreatment, but this reduction is not significant (mean ± SEM shown).

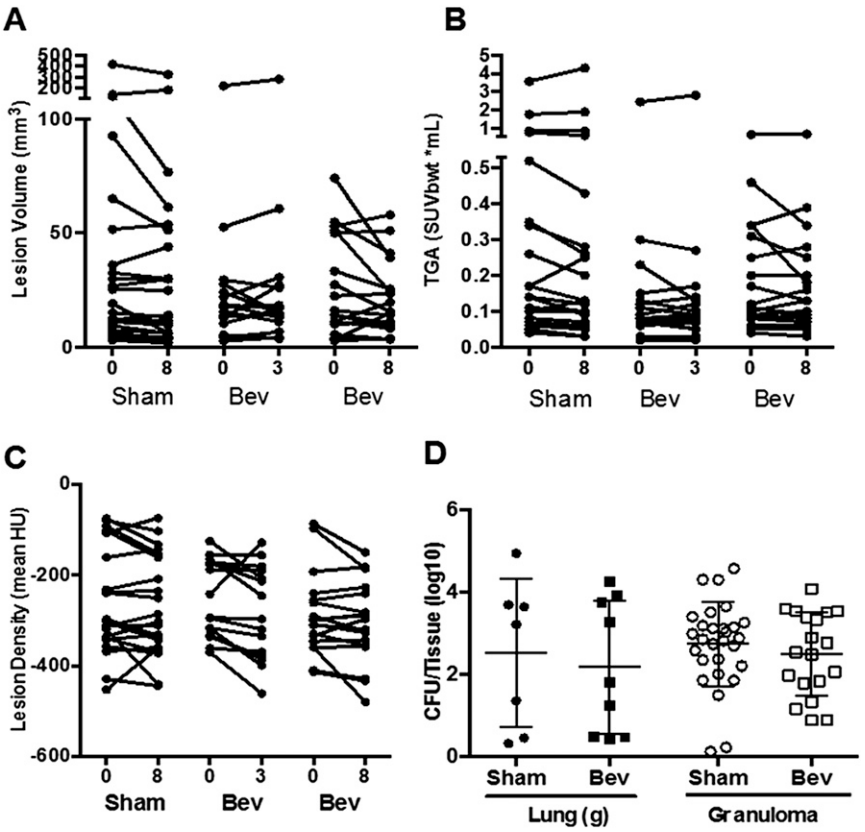

Fig. S3. Bevacizumab treatment does not affect lesion volume, density, FDG avidity, or bacterial load. Granuloma volume, density, and FDG uptake were measured in all identified parenchymal lesions in serial scans of each rabbit on the days indicated. The number of lesions per rabbit, as detected by FDG-PET/CT, ranged from 6 to 14 lesions, and all identified lesions were measured. TB granulomas are dynamic and change in both volume and FDG activity even in established infections (2). (*A*) Treatment with bevacizumab (Bev) did not affect lesion volume in comparison to sham-treated rabbits. (*B*) There was an insignificant trend toward increased FDG uptake in both bevacizumab-treated rabbit groups ($P = 0.09$). SUVbwt, standardized uptake value body weight. (*C*) Anti-VEGF treatment did not affect lesion density in comparison to sham-treated rabbits. HU, Hounsfield units. (*D*) Treatment with bevacizumab ($n = 5$ rabbits) compared with controls ($n = 4$ rabbits) did not affect bacterial load per gram in the whole-lobe homogenates [Lung (grams)] or individual granulomas, as assessed by cfu 8 d after bevacizumab treatment (mean ± SD shown).